Desalination and Water Treatment
www.deswater.com

doi: 10.5004/dwt.2018.23157

135 (2018) 408–417
December

Dynamic and static adsorption of phosphate in water on the zirconium oxychloride modified zeolite

Jianhua Yang[1], Min Yang[1], Hua Gui, Guizhen Li*, Hongbin Wang*

School of Chemistry and Environment, Key Laboratory of Resource Clean Conversion in Ethnic Regions, Yunnan Minzu University, Kunming 650500, China, email: 826677468@qq.com (M. Yang), 569684980@qq.com (H. Gui), 325865775@qq.com (G. Li), wanghb2152@126.com (H. Wang)

Received 18 July 2018; Accepted 16 September 2018

ABSTRACT

In this paper, the dynamic and static adsorption performance of phosphate in the water on the zirconium modified zeolite (Cl_2OZr/zeolite) was investigated. Batch adsorption experiments were performed to evaluate the adsorption conditions and selectivity. The experimental results agree well with the pseudo second-order kinetic model. The effects of the dynamic adsorption of phosphate on Cl_2OZr/zeolite were studied. The results indicate that the breakthrough time is 480 min and the phosphate removal rate reaches 95% under the optimal conditions. The curves of dynamic adsorption could be fitted by the Thomas model. Cl_2OZr/zeolite can be reused and applied to the actual waste water treatment. Comparing previous studies on phosphate removal with different adsorbents, we can see that the Cl_2OZr/zeolite has the advantages of wide pH range, relatively short adsorption equilibrium time and reusability.

Keywords: Phosphate; Zirconium oxychloride modified zeolite; Dynamic and static adsorption; Regeneration

1. Introduction

Phosphorus is an important ingredient for all living organisms and its application in agriculture as a fertilizer is necessary for production of food. The mining and use of phosphate rock has begun increased dramatically around the mid-to-late 19th century [1,2]. The data of substance flows analysis (SFA) through the food system by Cordell et al. [3] revealed that only one-fifth of applied phosphate fertilizer is assimilated by plants and animals [4–6]. Therefore, most of the phosphate is lost along the way of flow through the food production and consumption system, causing serious environmental problems particularly the worldwide eutrophication of lakes, reservoirs, estuaries, and parts of the oceans [7,8]. Phosphate is growth-nutrient for microorganisms present in water bodies. However, increased emissions of phosphate result in the excessive growth of photosynthetic aquatic micro- and macro-organisms and ultimately become a primary cause of eutrophication [9]. Thus, it is necessary to develop new methods for the removal of phosphate to prevent eutrophication. Heretofore, various methods have been developed for reduce of the phosphate in sewage discharge [10,11]. The phosphate removal techniques fall into three main categories physical, chemical, and biological. Physical methods have proven to be either too expensive (reverse osmosis and electrodialysis), or inefficient (removing only 10% of the total phosphorus (TP) [12]. Optimized biological treatment can remove up to 97% of TP; however, this efficiency can be highly variable because of operational difficulties, i.e. the trouble of maintaining the ideal anaerobic or aerobic state [13]. Additionally, the need to dispose large amounts of waste activated sludge limits the development of enhanced biological phosphorus (P)

*Corresponding author.

Presented at the 10th International Conference on Challenges in Environmental Science & Engineering (CESE-2017), 11–15 November 2017, Kunming, China.

removal techniques. Chemical removal techniques, such as adsorption and precipitation [57], have been considered as the most effective techniques for nutrient removal. Adsorption is one of the most investigated technologies for removal and recovery of phosphate from wastewater as recently studied [14–16], because of their relatively low costs, abundant adsorbent source materials (such as activated carbon [17–19,53], natural zeolites [20], and steel slag [21,58] and so on), and their simplicity of application to P recovery [22]. For this technique, phosphate is removed from wastewater via selective adsorption to a solid phase (adsorbent). The adsorbent may be reused again for phosphate capture after regeneration. Various coated adsorbents have been developed to remove phosphorous. However, the application of conventional adsorbent materials is limited by their low adsorption capacities, complicated implementation, and potential environmental risks. For example, the adsorption performances of granulated ferric hydroxide and activated aluminum oxide adsorbents are strongly dependent upon pH, and several anions (such as Cl^- and SO_4^{2-}) coexisting with phosphate in sewage [23]. The Cl_2OZr/zeolite was obtained by introducing zirconium and hydrated zirconia into the inner and outer surfaces of the zeolite to form an anionic active adsorption center. Therefore, the functional treatment of zeolite increases the adsorption capacity of anions [24].

In this study, a novel Cl_2OZr/zeolite is prepared for removing phosphate from Wastewater by static and dynamic adsorption tests. The influencing factors of contact time, pH of the solution, temperature, zeolite dose and co-existing anions on the batch adsorption behavior were studied. The kinetics of adsorption was analyzed using pseudo-first-order and pseudo-second-order kinetics models. The influences of the quantity of adsorbent, the filler particle size and flow rate in the fixed-bed column on dynamic adsorption performance were studied. The breakthrough curves for the adsorption of phosphate were analyzed by using Thomas model. In addition, reusability of the Cl_2OZr/zeolite was estimated. The Cl_2OZr/zeolite was also applied to the removal of phosphate in actual wastewater with satisfied results. Table 1 compares previous studies on phosphate removal with different adsorbents, we can see that the Cl_2OZr/zeolite has the advantages of wide pH range, relatively short adsorption equilibrium time and reusability.

2. Experiment

2.1. Materials

Natural zeolite was collected from Wenshan (Yunnan, China). Zirconium oxychloride octahydrate was purchased from Shanghai Chemical Reagent Company. Tartaric acid antimony potassium was obtained from Shanghai Heng Yuan Biotechnology Co., Ltd. Ammonium molybdate tetrahydrate was purchased from Shantou Xilong Chemical Factory. Lanthanum chloride heptahydrate (Tianjin Jinnan District salt water industrial park), Hexahydrate was obtained from Sinopharm Group Chemical Reagent Co., Ltd. Potassium dihydrogen phosphate was purchased from Tianjin Institute of Fine Chemical Industry. All other reagents were of analytical grade and used as received. Ultrapure water obtained from a Millipore filtration system was used throughout all experiments. The Cl_2OZr/zeolite was prepared according to our previous report [30].

2.2. Static adsorption studies

Batch experiments were carried out in the adsorption flask. The different amount of adsorbent was added into 50 mL 10 mg L^{-1} of phosphorus-containing wastewater. The pH of the aqueous solution was adjusted by 1 mol L^{-1} NaOH or 1 mol L^{-1} HCl and measured by a pH meter. The batch experiments were carried out at a thermostatic shaker for 60 min at 25°C. After centrifugation, the residual amount of phosphate in the supernatant was determined by molybdenum antimony scandium spectrophotometry.

Removal efficiency of phosphate was measured using following equation:

Table 1
Compare previous studies on phosphate removal with different adsorbents [25–29]

Adsorbent used	Type of wastewater used	Temp.	pH	Time	Percentage removal	Regeneration rate	Reference
Phosphate modified calcite	Synthetic solution	303K 313K 323K	5–7	2 h	72%	–	[21]
La(III)-loaded SOW	Synthetic solution	35°C	5–7	15 h	98.5%	85%	[22]
DETA-PES-Cu(II)	Synthetic solution	288K 298K 308K	5.1	300 min	–	–	[23]
CP-Fe-I	Actual water	30°C	2–5	200 min	–-	–	[24]
Cl_2OZr/zeolite	Actual water	25°C 35°C 45°C	2–8	2 h	81.56%	87.91%	Present study

$$R(\%) = \frac{(C_0 - C_t)}{C_0} \times 100 \quad (1)$$

where C_0 is initial concentration (mg L^{-1}), C_t is residual phosphate concentration after adsorption (mg L^{-1}) in solution.

The phosphate adsorption capacity Q (mg g^{-1}) was calculated by equation:

$$Q = \frac{(C_0 - C_t) \times V}{m \times 1000} \quad (2)$$

where V is the volume of waste water (mL), m is the amount of adsorbent (g).

2.2.1. Adsorption kinetic

The mechanism of the adsorption process is investigated through adsorption kinetics [31,32]. Two kinetic models, namely pseudo-first-order and pseudo-second-order models were used to test the experimental data [33]. The pseudo-first-order model is on the following assumption: the sorption rate abates linearly with the adsorption capacity. The pseudo-second-order kinetic model is usually utilized to elucidate a chemical sorption.

i. The pseudo-first-order kinetic model

The pseudo-first-order kinetic model was successfully applied to describe the kinetics of many adsorption systems. The pseudo-first-order rate equation is represented as below:

$$\text{In}\,(Q_e - Q_t) = \text{In}\,Q_e - k_1 t \quad (3)$$

where Q_e and Q_t are the amount of phosphate adsorbed (mg g^{-1}) at equilibrium and at t min, respectively. And k_1 (min^{-1}) is the rate constant of pseudo-first-order adsorption.

ii. The pseudo-second-order kinetic model

The adsorption kinetics may also be described by a pseudo-second-order kinetic model. The linearized integral form of the model is represented as:

$$\frac{t}{Q_t} = \frac{t}{Q_e} + \frac{1}{k_2 Q_e^{\,2}} \quad (4)$$

where k_2 (g mg^{-1} min^{-1}) is the equilibrium rate constant of pseudo-second-order adsorption. The pseudo-second-order model was based on the following assumptions [34]: (1) the adsorption followed the Langmuir isotherm, and (2) the limiting rate process is chemical adsorption, (3) the rate of occupation of adsorption sites is proportional to the square of number of unoccupied sites.

2.3. Dynamic adsorption studies

The fixed bed is adopted for the dynamic adsorption of the phosphate in water. It could not only improve the efficiency of the wastewater treatment, but also control the whole adsorption process via adjusting the quantity of adsorbent, the filler particle size, and flow rate. Column was packed with different amount of 10, 15 and 20 g of Cl_2OZr/zeolite as adsorbent. Furthermore, the effect of the filler particle size on removing rate of phosphate was investigated. The influent of flow rate (0.5, 2.0 and 3.0 mL min^{-1}) was also optimized.

The analysis of breakthrough curve data obtained from the bed dynamic process is essential in constructing an industrial wide range of adsorption process [35]. Breakthrough time was calculated at the point where effluent concentration ($C_{out,}$ mg L^{-1}) was about 1% of the influent concentration (C_{int}, mg L^{-1}) [36,37]. The adsorption capacity of phosphate was calculated by the breakthrough curve according to Eq. (5).

$$Q_t = \frac{10^{-3}\nu\int_0^t (C_{\text{int}} - C_{\text{out}})dt}{m} = \frac{10^{-3}\nu\left(C_{\text{int}}\, t - \int_0^t C_{\text{out}}\, dt\right)}{m} \quad (5)$$

where Q_t is the amount of adsorption at time t (mg g^{-1}), C_{int} is influent phosphate wastewater concentration (mg L^{-1}), C_{out} is effluent phosphate concentration (mg L^{-1}), t is adsorption time (min), v is flow rate (mg min^{-1}), $\int_0^t C_{out}$ is the area under the curve penetrated by t min.

It is assumed that there is no axial dispersion in column adsorption, so that the rate driving force obeys second order reversible kinetics. The model also estimates the relationship between concentration and time. The linearized form of the model is expressed as equation:

$$\text{In}\left(\frac{C_{\text{int}}}{C_{\text{out}}} - 1\right) = \frac{K_{Th} Q_e m}{\nu} - K_{Th} C_{\text{int}} t \quad (6)$$

where K_{Th} and Q_e are the Thomas kinetic constant (mL min^{-1} mg^{-1}) and equilibrium uptake capacities (mg g^{-1}), respectively. The values of K_{Th} and Q_e can be calculated from the plot of $\ln(C_{int}/C_{out} - 1)$ *vs.* time.

2.4. Desorption and reusability experiments

Because of OH influenced P adsorption to a great degree. Therefore, different NaOH concentrations were chosen to investigate the efficiency of desorption [38]. Saturated Cl_2OZr/zeolite was desorbed with the different concentrations of NaOH for regeneration. And the regenerated Cl_2OZr/zeolite was reused in adsorption experiment, and the regeneration process was repeated for two times.

3. Results and discussion

3.1. Static batch adsorption experiments

3.1.1. Effect of adsorbent dosage

The effect of zeolite dose on phosphate removal was explored at different dosages from 2 to 20 g L^{-1}. It is seen from Fig. 1 that the amount of phosphate adsorbed on

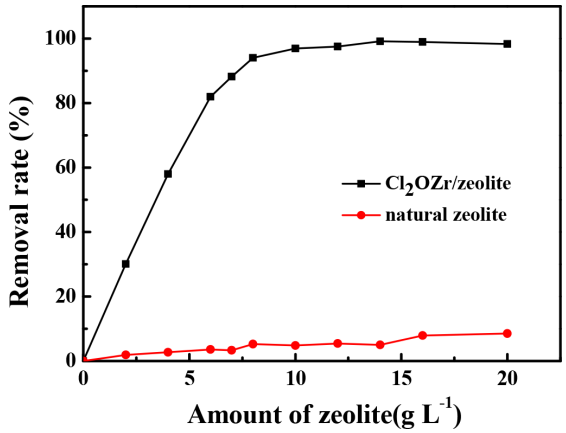

Fig. 1. The effect of the amount of Cl_2OZr/zeolite on the phosphate removal (experimental conditions: 50 mL 10 mg L^{-1} phosphorous-containing wastewater, 25°C, 200 rpm, shaking for 60 min).

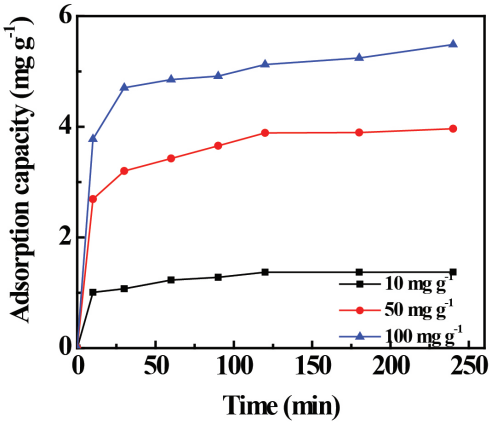

Fig. 2. The effect of contact time at different concentrations (experimental conditions: 50 mL 10 mg L^{-1} phosphorous-containing wastewater, 25–200 rpm, shaking for 10–240 min).

Cl_2OZr/zeolite increased with increasing zeolite dose and reached an equilibrium value at 7 g L^{-1} beyond which no more phosphate is further adsorbed from the solution. Phosphate removal was reduced from 10 mg L^{-1} to 1.2 mg L^{-1} with a dose of zeolite of 7 mg L^{-1}. The adsorption process is rapid at initial and became slow after the equilibrium. This might be due to increases in surface area of the adsorbent with increase in adsorbent dosage [39,52]. Greater availability of active sites and increment in surface area of the adsorbent with increase in adsorbent amount was also reported by Deng and Shi [40]. At this point, the amount of phosphate desorbed from Cl_2OZr/zeolite is in a state of dynamic equilibrium, which can meet the requirements of secondary emission standards of China's urban sewage treatment plant emission standards. Further, it was noticed that increased in adsorbent dose does not show any increase in removal efficiency. This may be due to fact that all active sites maybe occupied by the adsorbate at increase in dose [41]. The removal rate is increased slowly and flattens out gradually after a dosage of 7 g L^{-1}. Therefore, 7 g L^{-1} Cl_2OZr/zeolite was selected as the optimal amount of phosphorous-containing wastewater treatment experiments.

3.1.2 Effect of contact time and temperature

Fig. 2 shows the effect of contact time on phosphate adsorption with three different initial phosphate concentrations of 10, 50, 100 mg L^{-1} at 25°C. There is a fast phosphate adsorption during the first 60 min, which leads to a removal percentage of over 80% to three initial phosphate concentrations. The adsorption rate becomes slow subsequently, and reaches a plateau value. This is because the surface adsorption sites approach saturation as the contact time increases. In order to ensure that the amount of adsorption is closest to the equilibrium value, 120 min was selected as the equilibrium adsorption time [56,61,62]. The effect of temperature was also investigated at the 25°C, 35°C, and 45°C with an initial phosphate concentration of 10 mg L^{-1} as shown in Fig. 3. The temperature exhibits a little effect on the adsorption capacity and the equilibrium time. Thus, the temperature of 25°C was selected for further experiments.

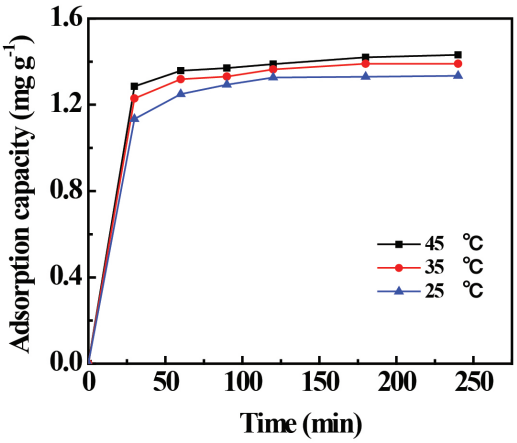

Fig. 3. The effect of contact time at different temperatures (experimental conditions: 50 mL 10 mg L^{-1} phosphorous-containing wastewater, 7 g L^{-1} Cl_2OZr/zeolite, 200 rpm, shaking for 10–240 min.

3.1.3. Effect of pH

The effect of the pH of the solution on phosphate removal is shown in Fig. 4. When the pH value is between 2.0 and 8.0, the amount of phosphate adsorbed on the Cl_2OZr/zeolite keeps higher adsorption ability and does not significantly change. When the pH > 8.0, the adsorbed amount was decreased quickly and reached the lowest value at the pH > 11.0. Higher adsorption capacity at lower pH can be because of the presence of H^+ ions [42,43]. On the other hand, at higher pH, decrease in adsorption could be attributed to higher concentration of Hydroxide ions and also due to Electrostatic attraction between the negatively charged ions [44–47,59]. Cl_2OZr/zeolite exhibits high phosphate removal efficiency over a wide pH range of 2.0–8.0.

3.1.4 Effect of co-existing ions

In general, phosphate contaminated water contains several other common anions like nitrate, carbonate, sulfate,

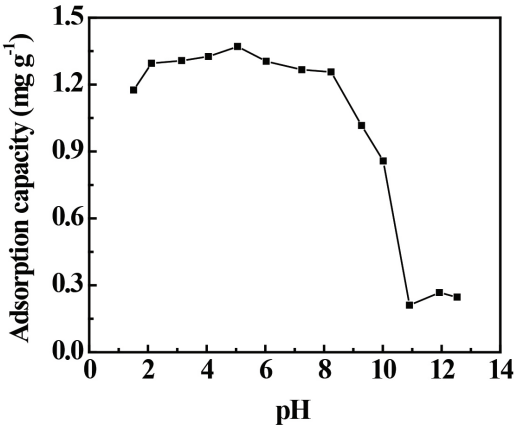

Fig. 4. Effect of the pH on the phosphate removal of Cl_2OZr/zeolite-experimental conditions: 50 mL 10 mg L^{-1}phosphorous-containing wastewater, 7 g L^{-1} Cl_2OZr/zeolite, 1 mol L^{-1} NaOH and 1mol L^{-1} HCl.

fluoride and chloride which can compete with phosphate in the adsorption process. In order to illustrate the effect of interfering anions, adsorption studies were carried out by varying the initial concentrations of co-existing anions from 50 to 500 mg L^{-1}. Adsorption of phosphate was studied in the presence of anions viz., F^-, Cl^-, CO_3^{2-}, SO_4^{2-}, and NO_3^- at given experimental conditions and results are shown in Fig. 5. The F^- and CO_3^{2-} display a competitive effect on the removal of phosphate by Cl_2OZr/zeolite, and other anions have no effect [63,64]. The CO_3^{2-} ion has effect on phosphate removal because CO_3^{2-} forms HCO_3^- in acidic water and competes with $H_2PO_4^-$ [48]. And F^- has a strong electronegativity and it is easily combined with the protonated adsorbent surface. Therefore, the adsorption capacity of phosphate is reduced [49,50,55].

3.1.5. Adsorption kinetic

The kinetic experiments were carried out under different phosphate concentration and temperature. The experimental data of Figs. 2 and 3 were fitted by the models

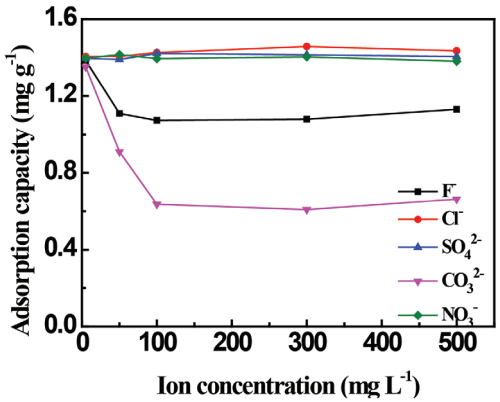

Fig. 5. Effect of co-existing anions on phosphate removal of Cl_2OZr/zeolite (experimental conditions: 50 mL 10 mg L^{-1} phosphorous-containing wastewater, 7 g L^{-1} Cl_2OZr/zeolite).

of the pseudo-first-order kinetic model and the pseudo-second-order kinetic model. The results were listed in Table 2. All the experimental data showed excellent compliance by the pseudo-second-order kinetic model with good correlation coefficients ($R > 0.9992$).

The adsorption kinetic followed the pseudo-second-order equation indicating that the limiting process of adsorption rate was chemical sorption [54]. The pseudo-second-order kinetic model contains all the processes such as liquid film diffusion, surface adsorption and intraparticle diffusion of phosphate adsorbed on the Cl_2OZr/zeolite. The initial adsorption rate constant sharply increases with the initial concentration increases. This is because Cl_2OZr/zeolite contains a large number of active sites in the early stage of adsorption. The greater the concentration gradient in solid-liquid systems with greater the concentration of adsorbates, so phosphate can easily propagate through the liquid film to the surface of Cl_2OZr/zeolite. The surface adsorption sites are nearly saturated with the reaction time increases. After this process, the adsorption rate decreases, due to the large mass transfer resistance.

3.2. Dynamic adsorption experiments

3.2.1. Effect of the filler particle size

Effect of particle size of Cl_2OZr/zeolite on the removal efficient of phosphate was investigated. The adsorption breakthrough curves were recorded with different particle size at amount of 10 g of adsorbent, flow rate of 3 mL min^{-1}, and phosphate concentration of 10 mg L^{-1}. It can be seen from Fig. 6 that more adsorption capacity of the Cl_2OZr/zeolite for the phosphate was observed at smaller particle size. The breakthrough time is 120, 300 and 390 min, and the penetration volume is 357, 890 and 1165 mL for particle sizes of 0.6–2.0, 0.30–0.45 and 0.2–0.3 mm, respectively. The effluent concentration of phosphate was below 1 mg L^{-1} and the corresponding penetrating adsorption capacity was 0.36, 0.87 and 1.15 mg g^{-1}, respectively. The equilibrium of adsorption was reached when the effluent concentration

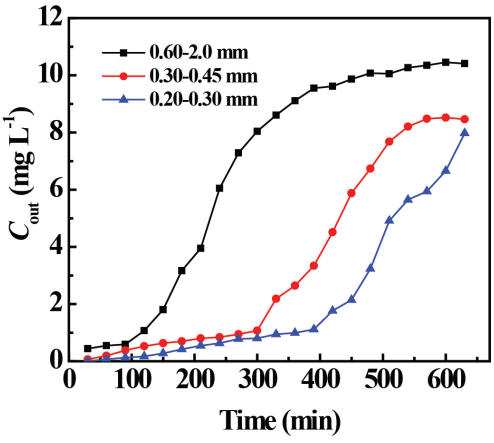

Fig. 6. Adsorption breakthrough curves at different particle sizes (experimental conditions: 50 mL 10 mg L^{-1} phosphorous-containing wastewater, 10 g Cl_2OZr/zeolite, the flow rate 3 mL min^{-1}).

Table 2
Correlation parameters of pseudo-first-order kinetic equation and pseudo-second-order kinetic equation

Variable	Measured Q_e (mg g^{-1})		Pseudo-first-order kinetics equation			Pseudo-second-order kinetics equation			
			Q_e (mg g^{-1})	k_1 (min^{-1})	R^2	Q_e (mg g^{-1})	h (mg/g min^{-1})	k_2 (g (mg $min)^{-1}$)	R^2
Phosphate concentration (mg L^{-1})	10	1.373	0.818	0.0351	0.9657	1.420	0.19	0.0945	0.9995
	50	3.964	1.404	0.0186	0.9559	4.087	0.49	0.0295	0.9996
	100	5.485	1.677	0.0121	0.9858	5.556	0.71	0.0231	0.9992
Temperature (K)	298	1.334	0.409	0.0276	0.9687	1.369	0.25	0.1351	0.9999
	308	1.392	0.366	0.0244	0.9600	1.421	0.28	0.1406	0.9999
	318	1.432	0.489	0.0254	0.9474	1.457	0.30	0.1417	0.9999

was below 95% of the initial concentration. The equilibrium times for adsorbent with different particle sizes were 480, 720 and 900 min, and the corresponding equilibrium adsorption capacities were 0.7, 1.36 and 1.65 mg g^{-1}, respectively. The shorter breakthrough time indicates that the packed column has low adsorption capacity. The strong adsorption capacity for small adsorbent particle size can be ascribed to more adsorption sites on adsorbent surface. So the smaller particle exhibits higher adsorption capacity and longer breakthrough time. The larger particle size displays a short breakthrough time because the porosity of the fixed-bed becomes larger and the resistance becomes smaller. Therefore, the filler particle size of 0.30–0.45 mm is selected in this experiment.

3.2.2. Effect of the quantity of adsorbent

Phosphate adsorption in a fixed-bed column system was associated with the quantity of adsorbent. In order to obtain phosphate removal effect at the different adsorbent quantity, the column was packed with 10, 15 and 20 g of Cl_2OZr/zeolite, respectively. The adsorption experiments were conducted using 10 mg L^{-1} phosphate solution. The breakthrough curves are shown in Fig. 7. A typical S curve was observed as the quantity of adsorbent grew larger. With the increase of the adsorbent quantity, the breakthrough time increased accordingly. The total adsorption capacity for three adsorbent quantities was 0.88, 0.96 and 1.05 mg g^{-1}. The adsorption capacity of the fixed-bed was increased with the increasing adsorbent quantity. This is due to the more specific surface of the adsorbent and more fixation binding sites. Basically, the increase of the adsorbent quantity in column would provide a larger effective area, which lead to an increase in the transfer zone from the entrance to the exit of the bed. Therefore, the increase in the quantity of adsorbent would broad the mass transfer zone and create a longer distance to reach the exit resulting in an extended breakthrough time. Comparing 15 g and 20 g of Cl_2OZr/zeolite increased the amount of adsorbent and the removal capacity was relatively small. Therefore, in this experiment, adsorbent quantity of 15 g was selected as the amount of filler in the adsorption column.

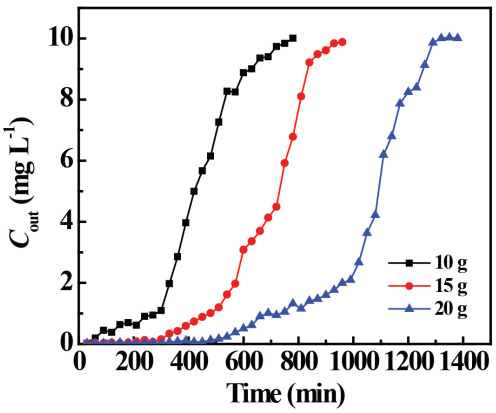

Fig. 7. Adsorption breakthrough curves at different quantity of adsorbent (experimental conditions: 50 mL 10 mg L^{-1} phosphorous-containing wastewater, the filler particle size of 0.30–0.45 mm, the flow rate 3 mL min^{-1}).

3.2.3. Effect of the flow rate

The flow rate of phosphate in a column affects the uptake capacity of the phosphate. In this study, the effect of flow rate was studied at the particle size is 0.30–0.45 mm, the quantity of 15 g and initial phosphate concentration of 10 mg L^{-1}. The breakthrough curves are presented in Fig. 8. According to Fig. 8, the breakthrough time were 690, 480 and 120 min, the breakthrough volumes were 675, 1430 and 2385 mL and the adsorption capacity was 1.36, 0.96 and 0.23 mg g^{-1}, respectively. The equilibrium adsorption time of the Cl_2OZr/zeolite were 1080, 930 and 480 min and the adsorption capacity were 1.64, 1.42 and 0.51 mg g^{-1} at flow rates of 1.0, 3.0, and 5.0 mL min^{-1}, respectively. At higher flow rates, the phosphates stay in the column for a relatively shorter time resulting in less efficient in contacting and reacting with the Cl_2OZr/zeolite and early breakthrough and saturation of the column. So, the Cl_2OZr/zeolite capacity decreases with increasing flow rate due to the insufficient residence time of phosphate in the column, which indicates that better column performance can be obtained at a lower flow rate. However, too small flow rate

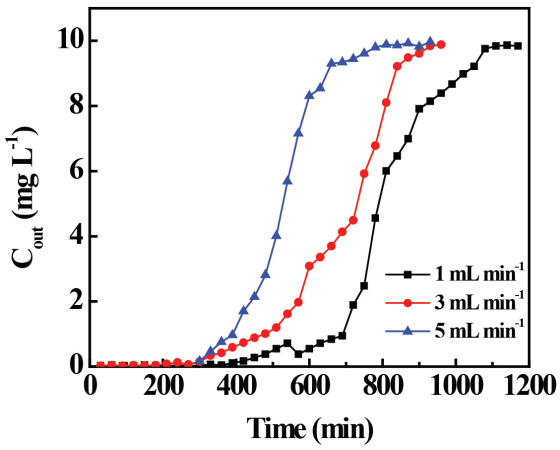

Fig. 8. Breakthrough curves at different flow rates (experimental conditions: 50 mL 10 mg L^{-1} phosphorous-containing wastewater, the filler particle size of 0.30–0.45 mm, 15 g Cl_2OZr/zeolite).

results in small amount of wastewater treatment and long processing time [51]. Therefore, we selected 3 mL min^{-1} as the flow rate.

3.2.4. The Thomas model

The breakthrough curves for the absorption of phosphate onto Cl_2OZr/zeolite were analyzed using the Thomas model. The parameters K_{Th} and Q_e and correlation coefficient (R) were determined and as shown in Table 3. From Table 3, the K_{Th} value decreases with the particle size and flow rate decreases and the quantity of adsorbent increases. The calculated value Q_e from the Thomas model is close to the experimental value Q. Thus, the linearized Thomas model can be used to describe the experimental breakthrough data adequately. Excellent R values from Thomas model indicate a good applicability of Thomas model. There is a good agreement between experimental and calculated adsorption capacities. These results indicate that the Thomas model perfectly described the phosphate breakthrough curve model.

3.3. Regeneration

3.3.1. Effect of the NaOH concentration

The saturated Cl_2OZr/zeolite can be regenerated by NaOH solution. The effect of NaOH concentration from 0.05 to 1.0 mol L^{-1} on the regeneration is shown in Fig. 9. It can be clearly seen that the regenerated capacity of Cl_2OZr/zeolite increases with the increase of NaOH concentration and reaches the maximum at 0.3 mol L^{-1} NaOH with regeneration capacity of 0.959 mg g^{-1} and regeneration rate of 63.37%. After optimal concentration of 0.3 mol L^{-1} NaOH, the regeneration capacity decreases because the regeneration ambient is destroyed by the excessive alkalinity, resulting a low regeneration performance. In subsequent experiments, 0.3 mol L^{-1} NaOH was selected for Cl_2OZr/zeolite.

3.3.2. Effect of the regeneration time

The effect of the regeneration time on the regenerated capacity of saturated Cl_2OZr/zeolite is shown in Fig. 10. According to Fig. 10, the regeneration capacity gradually

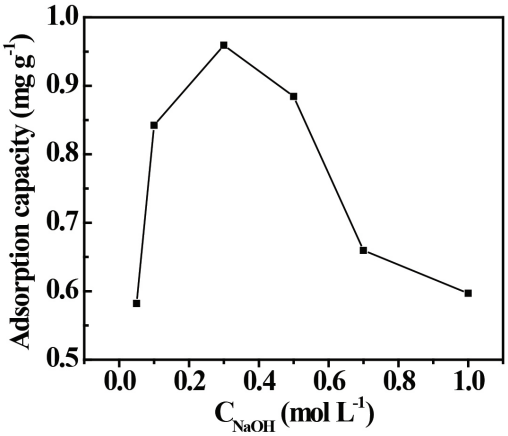

Fig. 9. Effect of the NaOH concentrations (experimental conditions: 25 g L^{-1} Saturated Cl_2OZr/zeolite, Solid-liquid ratio – 1:40 (g mL^{-1}), regeneration – 1 h).

Table 3
Thomas model fitting related parameters of different particle size, quantity of adsorbent and flow rate

Size (mm)	v (mL min)	m (g)	K_{Th} (mL (mg·min)$^{-1}$)	Q_e (mg g^{-1})	Experiment Q (mg g^{-1})	R^2
0.60–2.0	3	10	1.21	0.81	0.76	0.9844
0.30–0.45	3	10	1.00	1.37	1.36	0.9906
0.20–0.30	3	10	0.98	1.65	1.65	0.9923
0.30–0.45	3	10	1.07	1.38	1.35	0.9849
0.30–0.45	3	15	1.01	1.40	1.42	0.9902
0.30–0.45	3	20	0.78	1.58	1.63	0.9725
0.30–0.45	1	15	0.99	1.62	1.64	0.9768
0.30–0.45	3	15	1.01	1.40	1.42	0.9903
0.30–0.45	5	15	1.30	0.55	0.51	0.9793

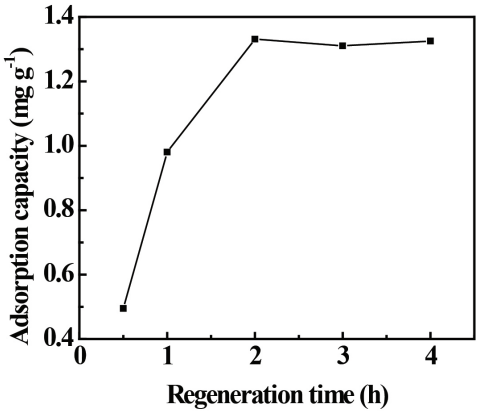

Fig. 10. Effect of regeneration time (experimental conditions: 25 g L^{-1} Saturated Cl_2OZr/zeolite, 0.3 mol L^{-1} NaOH).

increased with the regeneration time, and tends to be equilibrium after 2 h. The regeneration capacity was 1.331 mg g^{-1} and the regeneration rate was 87.91%. In this study, 2 h was selected as the regeneration time of Cl_2OZr/zeolite.

3.3.3. Elution curve

The recycling of adsorbent is very important for practical application. The regeneration capacity of the Cl_2OZr/zeolite as shown in Fig. 11. Phosphate solution was flowed through the Cl_2OZr/zeolite column with a constant flow rate of 1 mL min^{-1} and an inlet phosphate concentration of 10 mg L^{-1}. Then saturated Cl_2OZr/zeolite was subjected to desorption with 0.3 mol L^{-1} NaOH solution as the eluting agent. It is seen from Fig. 11 that the elution process is complete within 4 h and the ion exchange rate is fast. Low concentration of exit phosphate indicates that the saturated Cl_2OZr/zeolite column was eluted and regenerated.

3.3.4. Recycle column

The dynamic adsorption test was carried out after first and second regeneration of Cl_2OZr/zeolite column with 15 g Cl_2OZr/zeolite at flow rate of 3 mL min^{-1} and phosphate wastewater concentration of 10 mg L^{-1}. It can be seen from Fig. 12 that penetration time shifts to the left with increasing regenerative times. The breakthrough time was 390 and 360 min for 1st and 2nd times regeneration, and the corresponding penetration absorption capacity was 0.78 and 0.71 mg g^{-1}, respectively. The equilibrium adsorption time was 660 and 540 min, and the corresponding equilibrium adsorption capacity was 1.02 and 0.87 mg g^{-1}, respectively. The adsorption capacity decreased slightly compared with a fresh Cl_2OZr/zeolite column. This result indicates an excellent performance of regeneration for Cl_2OZr/zeolite column [60].

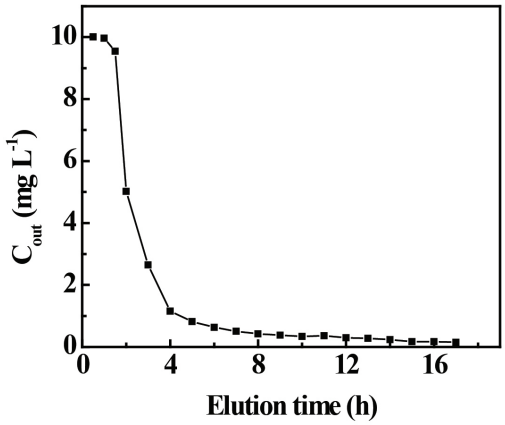

Fig. 11. Elution curve of the Cl_2OZr/zeolite column dynamic (experimental conditions: 25 g L^{-1} Saturated Cl_2OZr/zeolite, 0.3 mol L^{-1} NaOH, the flow rate 1 mL min^{-1}).

3.4. Practical application

To evaluate the practicality and usability of developed Cl_2OZr/zeolite column for phosphate removal, real water samples are investigated. The water samples are collected from the Chenggong Sewage Treatment Plant incoming and outgoing water in Kunming. The experimental results are listed in Table 4. It can be seen from Table 4 that the Cl_2OZr/zeolite column exhibits good removal rate for phosphorus-containing sewage. After treatment with Cl_2OZr/zeolite, the phosphate concentration of water samples is less than 0.5 mg L^{-1}, which lower the first-grade standard in the "Discharge Standard of Pollutants for Municipal Wastewater Treatment Plants" (GB18918-2002) and requires the water quality standard of reused landscape water (CJ/T95 -2000).

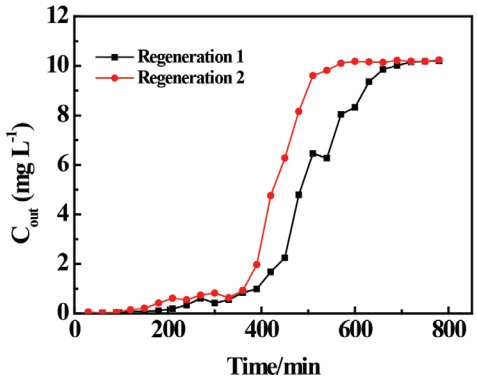

Fig. 12. Effect of regeneration times (experimental conditions: 50 mL 10 mg L^{-1} phosphorous-containing wastewater, the filler particle size of 0.30–0.45 mm, 0.3 mol L^{-1} NaOH, regeneration time 2 h).

Table 4
Results of removing phosphate in waste water using ZrO_2/zeolite

Samples	pH	C_{int} (mg L^{-1})	C_{out} (mg L^{-1})	Removal rate (%)
Incoming water	7.22	3.04	0.37	87.84
Outgoing water	7.24	0.44	0.08	81.56

4. Conclusions

In this work, dynamic and static removal of phosphate from water was investigated based on Cl_2OZr/zeolite composite material. Cl_2OZr/zeolite exhibits high adsorption capacity and excellent regeneration property for removal phosphate. The experimental conditions, including adsorbent dosage, contact time and temperature, solution pH, co-existing ions, filler particle size, quantity of adsorbent, and flow rate were optimized. The pseudo-second-order kinetic can well describe the behavior of the Cl_2OZr/zeolite for phosphate adsorption. And the dynamic adsorption behavior of the Cl_2OZr/zeolite can be described by the Thomas model. Regeneration performance of Cl_2OZr/zeolite column, including NaOH concentration, regeneration time, elution time, and recycle times were also studied. The experimental results indicate that Cl_2OZr/zeolite exhibits excellent adsorption capacity and regeneration properties. Cl_2OZr/zeolite was successfully applied for the removal of phosphate from real water samples with satisfied results.

Acknowledgments

This work was financially supported by YMU-DEAKIN International Associated Laboratory on Functional Materials, Education Department of Yunnan Province (117-02001001002107), College Student Innovation and Entrepreneurship Training Project of China (201710691001, and 201610691002).

References

[1] V. Smil, Phosphorus in the environment: Natural flows and human interferences, Annu. Rev. Energy Environ., 25(1) (2000) 53–88.
[2] D. Cordell, J.O. Drangert, S. White, The story of phosphorus: global food security and food for thought, Global Environ. Chang., 19(2) (2009) 292–305.
[3] J. Driver, D. Lijmbach, I. Steen, Why recover phosphorus for recycling, and how?, Environ. Technol. Letters, 20(7) (1999) 651–662.
[4] S. Taktek, M. Trépanier, P.M. Servin, M. St–Arnaud, Y. Piché, J.A. Fortin, Trapping of phosphate solubilizing bacteria on hyphae of the arbuscular mycorrhizal fungus rhizophagus irregularis, daom 197198, Soil Biol. Biochem., 90 (2015) 1–9.
[5] M.A. Whitelaw, T.J. Harden, K.R. Helyar, Phosphate solubilisation in solution culture by the soil fungus penicillium radicum, Soil Biol. Biochem., 31(5) (1999) 655–665.
[6] C. Mander, S. Wakelin, S. Young, L. Condron, M. O'Callaghan, Incidence and diversity of phosphate–solubilising bacteria are linked to phosphorus status in grassland soils, Soil Biol. Biochem., 44(1) (2012) 93–101.
[7] R. Perciasepe, National Strategy for the Development of Regional Nutrient Criteria. Office of Water U.S. Environ. Protection Agency, 35 (1998) 785–792.
[8] B.E. Rittmann, B. Mayer, P. Westerhoff, M. Edwards, Capturing the lost phosphorus, Chemosphere, 84(6) (2011) 846.
[9] R. Jeppesen, M. Rodriguez, J. Rinde, J. Haskins, B. Hughes, L. Mehner, Effects of hypoxia on fish survival and oyster growth in a highly eutrophic estuary, Estuaries Coasts, 41(1) (2018) 89–98.
[10] I.C.S. Duarte, L.L.D. Oliveira, D.Y. Okada, P.F.D. Prado, M.B.A. Evaluation of the microbial diversity in sequencing batch reactor treating linear alkylbenzene sulfonate under denitrifying and mesophilic conditions using swine sludge as inoculum, Brazilian Arch. Biol. Techn., 58(3) (2015) 326–332.
[11] W. Rast, J.A. Thornton, Trends in eutrophication research and control, Hydrol. Process., 10(2) (2015) 295–313.
[12] A. Luptakova, S. Ubaldini, E. Macingova, P. Fornari, V. Giuliano, Application of physical–chemical and biological–chemical methods for heavy metals removal from acid mine drainage, Process Biochem., 47 (2012) 1633–1639.
[13] A. Akcil, S. Koldas, Acid mine drainage (AMD): causes, treatment and case studies, J. Clean. Prod., 14 (2016) 1139–1145.
[14] G.K. Morse, S.W. Brett, J.A. Guy, J.N. Lester, Review: phosphorus removal and recovery technologies, Sci. Total Environ., 212 (1998) 69–81.
[15] L.E. De–Bashan, Y. Bashan, Recent advances in removing phosphorus from wastewater and its future use as fertilizer, Water Res., 38 (2004) 4222–46.
[16] L.A. Wendling, P. Blomberg, T. Sarlin, O. Priha, M. Arnold, Phosphorus sorption and recovery using mineral–based materials: sorption mechanisms and potential phytoavailability, Appl. Geochem., 37 (2013) 157–169.
[17] A. Dabrowski, P. Podkościelny, Z. Hubicki, M. Barczak, Adsorption of phenolic compounds by activated carbon––a critical review, Chemosphere, 58 (2005) 1049.
[18] B.H. Hameed, A.T. Din, A.L. Ahmad, Adsorption of methylene blue onto bamboo–based activated carbon: kinetics and equilibrium studies, J. Hazard. Mater., 141 (2007) 819–825.
[19] X. Fang, G. Li, J. Li, H. Jin, J. Li, V. Jegatheesan, S. Li, H.B. Wang, M. Yang, Bamboo charcoal derived high–performance activated carbon via microwave irradiation and KOH activation: application as hydrogen storage and super–capacitor, Desal. Water Treat., 96 (2017) 120–127.
[20] A.H. Oren, A. Kaya, Factors affecting adsorption characteristics of Zn^{2+} on two natural zeolites, J. Hazard. Mater., 131 (2006) 59–65.
[21] N.M. Reza, O. Sasan, Absorption of lead ions by various types of steel slag, Iran. J. Chem. Eng., 27 (2008) 69–75.
[22] B.K. Biswas, K. Inoue, K.N. Ghimire, S. Ohta, H. Harada, K. Ohto, The adsorption of phosphate from an aquatic environment using metal–loaded orange waste, J. Colloid Interf. Sci., 312 (2007) 214–223.
[23] L. Song, J. Huo, X. Wang, F. Yang, J. He, C. Li, Phosphate adsorption by a Cu(II)–loaded polyethersulfone–type metal affinity membrane with the presence of coexistent ions, Chem. Eng. J., 284 (2016) 182–193.
[24] K.A. Krishnan, A. Harida, Removal of phosphate from aqueous solutions and sewage using natural and surface modified coir pith, J. Hazard. Mater., 152 (2008) 527–535.
[25] L. Jiang, J.Y. Chen, X.M. Li, J. Luo, Q. Yang, Y. Wang, Adsorption of phosphate from wastewater by fly ash ceramsite, J. Environ. Sci., 31(7) (2011) 1413–1420.
[26] W.J. Zheng, J.W. Lin, Y.H. Zhan, H. Wang, Adsorption characteristics of nitrate and phosphate from aqueous solution on zirconium–hexadecyltrimethylammonium chloride modified activated carbon, Huanjing kexue, 36(6) (2015) 2185–2194.
[27] F. Haghseresht, S. Wang, D.D. Do, A novel lanthanum–modified bentonite, Phoslock, for phosphate removal from wastewaters, Appl. Clay Sci., 46(4) (2009) 369–375.
[28] X. Xiong, K.E. Fan, L.I. Yong, L.I. Wenchao, J. Pan, H. Zhang, Low concentration of phosphorus removal in waters with CaO_2, J. Lake Sci., 27(3) (2015) 493–501.
[29] Z. Duan, G. Li, L. Zhou, H. Gui, W. Tan, V. Jegatheesan, H.B. Wang, M. Yang, Preparation of zeolite–based zirconium functional materials (Ze–Zr) with the aid of response surface methodology, Process Saf. Environ., 112 (2017) 353–361.
[30] F. Zhao, W.Z. Tang, D. Zhao, Y. Meng, D. Yin, M. Sillanpää, Adsorption kinetics, isotherms and mechanisms of Cd(II), Pb (II), Co(II) and Ni(II) by a modified magnetic polyacrylamide microcomposite adsorbent, J. Water Process Eng., 4 (2014) 47–57.
[31] N.N. Nassar, A. Hassan, G. Vitale, Comparing kinetics and mechanism of adsorption and thermo–oxidative decomposition of Athabasca asphaltenes onto TiO_2, ZrO_2, and CeO_2 nanoparticles, Appl. Catal. A: General, 484 (2014) 161–171.

[32] R. Wang, G. Li, Y. Yang, L. Shu, V. Jegatheesan, H.B. Wang, M. Yang, Study on the adsorption performance for fluoride by mesoporous silica loaded rare earth lanthanum (Ms–La) material, Desal. Water Treat., 96 (2017) 104–111.
[33] R. Radhika, T. Jayalatha, S. Jacob, R. Rajeev, B.K. George, B.R. Anjali, Removal of perchlorate from drinking water using granular activated carbon modified by acidic functional group: Adsorption kinetics and equilibrium studies, Process Safety Environ., 109 (2017) 158–171.
[34] R. Wang, L. Luo, Y. JunYang, L. Shu, V. Jegatheesan, H.B. Wang, M. Yang, Preparation and characterization of mesoporous silica (Ms) supporting lanthanum carbonate (Ms–La) for the defluorination of aqueous solutions, Desal. Water Treat., 96 (2017) 112–119.
[35] D. Pokhrel, T. Viraraghavan, Arsenic removal in an iron oxide–coated fungal biomass column: analysis of breakthrough curves, Bioresour. Technol., 99 (2008) 2067–2071.
[36] B.C. Pan, F.W. Meng, X.Q. Chen, B.J. Pan, X.T. Li, W.M. Zhang, Y. Sun, Application of an effective method in predicting breakthrough curves of fixed–bed adsorption onto resin adsorbent, J. Hazard. Mater., 124 (2005) 74–80.
[37] W. Gu, X. Li, M. Xing, W. Fang, D. Wu, Removal of phosphate from water by amine–functionalized copper ferrite chelated with La(III), Sci. Total Environ., 619–620 (2018) 42.
[38] S. Mor, K. Ravindra, N.R. Bishnoi, Adsorption of chromium from aqueous solution by activated alumina and activated charcoal, Biores. Technol., 98(4) (2007) 954–957.
[39] D. Lin, Z. Shi, Synthesis and characterization of a novel Mg–Al hydrotalcite–loaded kaolin clay and its adsorption properties for phosphate in aqueous solution, J. Alloy. Comp., 637 (2015) 188–196.
[40] J.B. Xiong, Z.l. He, D. Liu, Phosphate removal from solution using steel slag through magnetic separation, J. Hazard. Mater., 152(1) (2008) 211–215.
[41] K. Kaur, S. Mor, K. Ravindra, Removal of chemical oxygen demand from landfill leachate using cow–dung ash as a low–cost adsorbent, J. Colloid Interf. Sci., 469 (2016) 338–343.
[42] G. Zelmanov, R. Semiat, Phosphate removal from aqueous solution by an adsorption ultrafiltration system, Sep. Purif. Technol., 132(34) (2014) 487–495.
[43] A. Ahmad, M. Rafatullah, O. Sulaiman, M.H. Ibrahim, C. Yapyee, Removal of Cu(II) and Pb(II) ions from aqueous solutions by adsorption on sawdust of Meranti wood, Desalination, 247(1) (2009) 636–646.
[44] S. Mor, K. Chhoden, K. Ravindra, Application of agro–waste rice husk ash for the removal of phosphate from the wastewater, J. Clean. Prod., 129 (2016) 673–680.
[45] Y.J. Xue, H.B. Hou, S.J. Zhu, Characteristics and mechanisms of phosphate adsorption onto basic oxygen furnace slag, J. Hazard. Mater., 162(2) (2009) 973–980.
[46] R. Li, J.J. Wang, B. Zhou, M.K. Awasthi, A. Ali, Z. Zhang, Enhancing phosphate adsorption by Mg/Al layered double hydroxide functionalized biochar with different Mg/Al ratios, Sci. Total Environ., 559 (2016) 121–129.
[47] K. Peng, H. Kong, D .Zhang, D. Wu, H. Pang, Effect of several common ions on phosphate removal by detoxification chromium slag, Technol. Water Treat., (2009).
[48] G. Li, S. Gao, G. Zhang, X. Zhang, Enhanced adsorption of phosphate from aqueous solution by nanostructured iron(III)–copper(II) binary oxides, Chem. Eng. J., 235(1) (2014) 124–131.
[49] R. Li, J.J. Wang, B. Zhou, M.K. Awasthi, A.A. li, Z. Zhang, A. Mahar, Enhancing phosphate adsorption by Mg/Al layered double hydroxide functionalized biochar with different Mg/Al ratios, Sci. Total Environ., 559 (2016) 121–129.
[50] T.A. Nguyen, H.H. Ngo, W.S. Guo, T.Q. Pham, F.M. Li, T.V. Nguyen, Adsorption of phosphate from aqueous solutions and sewage using zirconium loaded okara (ZLO): fixed–bed column study, Sci. Total Environ., 523 (2015) 40–49.
[51] J.W. Lin, J. Li, Y.H. Zhan, Study on removal of phosphate in water by phosphate modified calcite, J. Eco–Environ., 9 (2013) 1594–1601.
[52] L. Jiang, J.Y. Chen, X.M. Li, J. Luo, Q. Yang, Y. Wang, Adsorption of phosphate from wastewater by fly ash ceramsite, J. Environ. Sci., 31(7) (2011) 1413–1420.
[53] W.J. Zheng, J.W. Lin, Y.H. Zhan, H. Wang, Adsorption characteristics of nitrate and phosphate from aqueous solution on zirconium–hexadecyltrimethylammonium chloride modified activated carbon, Huanjing kexue, 36(6) (2015) 2185–2194.
[54] F. Haghseresht, S. Wang, D.D. Do, A novel lanthanum–modified bentonite, Phoslock, for phosphate removal from wastewaters, Appl. Clay Sci., 46(4) (2009) 369–375.
[55] X. Xiong, K.E. Fan, L.I. Yong, L.I. Wenchao, J. Pan, H. Zhang, Low concentration of phosphorus removal in waters with CaO_2, J. Lake Sci., 27(3) (2015) 493–501.
[56] S. Mor, K. Ravindra, N.R. Bishnoi, Adsorption of chromium from aqueous solution by activated alumina and activated charcoal, Biores. Technol., 98(4) (2007) 954–957.
[57] D. Lin, Z. Shi, Synthesis and characterization of a novel Mg–Al hydrotalcite–loaded kaolin clay and its adsorption properties for phosphate in aqueous solution, J. Alloy. Comp., 637 (2015) 188–196.
[58] J.B. Xiong, Z.l. He, D. Liu, Phosphate removal from solution using steel slag through magnetic separation, J. Hazard. Mater., 152(1) (2008) 211–215.
[59] K. Kaur, S. Mor, K. Ravindra, Removal of chemical oxygen demand from landfill leachate using cow–dung ash as a low–cost adsorbent, J. Colloid Interf. Sci., 469 (2016) 338–343.
[60] G. Zelmanov, R. Semiat, Phosphate removal from aqueous solution by an adsorption ultrafiltration system, Sep. Purif. Technol., 132(34) (2014) 487–495.
[61] A. Ahmad, M. Rafatullah, O. Sulaiman, M.H. Ibrahim, C. Yapyee, Removal of Cu(II) and Pb(II) ions from aqueous solutions by adsorption on sawdust of Meranti wood, Desalination, 247(1) (2009) 636–646.
[62] S. Mor, K. Chhoden, K. Ravindra, Application of agro–waste rice husk ash for the removal of phosphate from the wastewater, J. Clean. Prod., 129 (2016) 673–680.
[63] Y.J. Xue, H.B. Hou, S.J. Zhu, Characteristics and mechanisms of phosphate adsorption onto basic oxygen furnace slag, J. Hazard. Mater., 162(2) (2009) 973–980.
[64] K. Peng , H. Kong , D. Zhang, D. Wu, H. Pang, Effect of several commonions on phosphate removal by detoxification chromium slag, Technol. Water Treat., (2009).